Femtosecond Pump-Probe Diagnostics of Preformed Plasma Channels

R. Zgadzaj, E. W. Gaul, N. H. Matlis, G. Shvets, A. Debus, and M. C. Downer

Articles you may be interested in

Measurement of thermal modulation of optical absorption in pump-probe spectroscopy of semiconducting polymers
Appl. Phys. Lett. 98, 223304 (2011); 10.1063/1.3595340

Pump-probe imaging of nanosecond laser-induced bubbles in distilled water solutions: Observations of laser-produced-plasma
J. Appl. Phys. 108, 103106 (2010); 10.1063/1.3506657

Nonlinear propagation of ultraintense and ultrashort laser pulses in a plasma channel limited by metallic walls
Phys. Plasmas 13, 083107 (2006); 10.1063/1.2219431

Diagnostic of Laser-Plasmas: Single-shot Supercontinuum Spectral Interferometry
AIP Conf. Proc. 737, 407 (2004); 10.1063/1.1842571

Development of a multichord beam-attenuation probe of hydrogen and helium for plasma diagnostics
Rev. Sci. Instrum. 70, 865 (1999); 10.1063/1.1149280

Femtosecond Pump-Probe Diagnostics of Preformed Plasma Channels

R. Zgadzaj, E. W. Gaul, N. H. Matlis, G. Shvets, A. Debus,
and M. C. Downer

University of Texas at Austin,
Department of Physics
Austin, TX 78712-1081

Abstract. We report on recent ultrafast pump-probe experiments[28] in He plasma waveguides using 800 nm, 80 fs pump pulses of 0.2x1018 W/cm2 peak guided intensity, and single orthogonally-polarized 800 nm probe pulses with ~0.1% of pump intensity. The main results are: (1) We observe frequency-domain interference between the probe and a weak, depolarized component of the pump that differs substantially in mode shape from the injected pump pulse; (2) we observe spectral blue-shifts in the transmitted probe that are not evident in the transmitted pump. The evidence indicates that pump depolarization and probe blue-shifts both originate near the channel entrance.

INTRODUCTION

Preformed plasma waveguides capable of controllably guiding relativistically intense fs laser pulses over multiple Rayleigh lengths without optical distortion are essential to developing GeV-scale laser wakefield accelerators and coherent short-wavelength sources.[1] Single pulses with peak intensity as high as $\sim 10^{17}$ W/cm^2 have been guided through plasma channels generated by different techniques.[2-9] We recently reported distortion-free guiding of single 80 fs pulses over $60z_R$ (1.5 cm) at $I_{guided} \simeq 2 \times 10^{17}$ W/cm^2 in a fully ionized Milchberg[6]-type channel in a He backfill.[7]

In this work we extend the previous study by reporting fs pump-probe experiments with pump intensity $I_{guided} \simeq 2 \times 10^{17}$ W/cm^2 in the fully ionized He channel. We show that, a simplified single probe implementation of FDI is possible for $\lambda_{probe} = \lambda_{pump}$, using either intentionally leaked pump or its naturally depolarized component produced in the interaction with the channel. This technique eliminates group velocity mismatch between pump and probe (which limits the usefulness of two-color techniques[13,15,19] in long interaction distances in channels), simplifies alignment by avoiding the need for a second reference probe, and is self calibrating in pump-probe time delay. In this paper we focus on the depolarized component of the pump because of its importance as an unavoidable background in pump-probe experiments and as a diagnostic of the channel and its entrance/exit regions. Our current experiments also illustrate the use of ionization-induced blue-shift $\Delta\lambda_{probe}$ to complement FDI as a diagnostic of probe pulse propagation through a channel at small Δt, where FDI fringes are too widely separated to be useful.

EXPERIMENTAL SETUP

Our procedure for generating, characterizing and guiding intense fs laser pulses through fully-ionized He channels has been described previously.[7] Channels are created by sending 400 ps, 1 J Nd:YAG laser pulses through an axicon lens into a 400 Torr He backfill. The resulting 1-cm-long line focus ionizes and heats the gas, driving a cylindrical shockwave radially outward. Fig.1 summarizes our diagnostic measurements of the channels and guided pump pulses used for the present pump-probe experiments.

Probe pulses $I_{probe} \simeq 10^{-3} I_{pump}$ were split from the pump (800nm, 80fs, 50mJ), passed through a variable delay, rotated in polarization by 90°, then recombined with the pump at a thin film polarizer. An f/10 off-axis parabolic mirror focused the co-propagating, orthogonally-polarized pump and probe pulses to the channel entrance. Light exiting the channel passed through a high-contrast (extinction ratio $\sim 10^{-6}$) calcite polarizer oriented parallel to the incident probe polarization (hereafter the x-direction), and was imaged with 100x magnification onto the entrance slit of an imaging spectrometer oriented along the x-direction (see Fig. 2a). A CCD detector recorded single-shot probe (+ pump leakage) spectra with $\sim 1\mu m$ spatial resolution along the x-direction, parallel to the slit. Good signal-to-noise ratio required a slit width of $\sim 500~\mu m$, which collected $\sim 1/3$ of the FWHM of the imaged mode. The present results were obtained with the slit located on average slightly off of the imaged mode center, as shown in Fig. 2a.

Propagating through vacuum, probe and leaked pump yielded flat, untilted reference FDI fringes, with a minimum modulation of $2\left|E_{leakage}^{\min}\right|/\left|E_{probe}\right| \approx 0.05$ corresponding to $\left|E_{leakage}^{\min}\right|/\left|E_{pump}\right| \approx 0.8 \times 10^{-3}$ (consistent with 10^{-6} polarizer extinction ratio). (Details of the experimental setup are found in ref. 28).
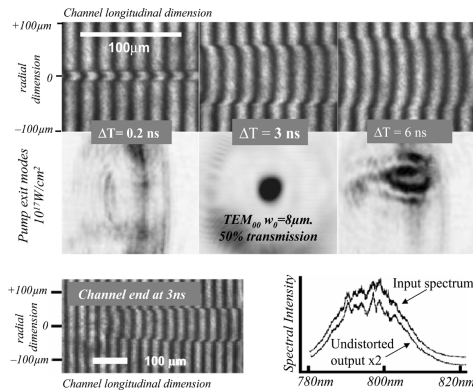

FIGURE 1. *Top row*) Transverse Mach-Zender interferograms of the expanding plasma channel at three time delays after the arrival of the channel forming pulse. *Middle row*) Modes of the exiting pump pulse shown below the corresponding interferograms. *Bottom left*) Transverse interferogram of the channel entrance. *Bottom right*) Spatially integrated spectra of the input and output pump pulses at $I_{guided} = 2 \times 10^{17}$ W/cm^2. Optimal guiding occurs at 3ns with 50% throughput at $I_{guided} = 2 \times 10^{17}$ W/cm^2.

EXPERIMENTAL RESULTS AND DISCUSSION

For channeling experiments, the chamber was filled with He gas, a channel was produced and the object plane of the imaging system was moved to the channel exit. Fig.2b shows single-shot, spatially-resolved spectra of $E_{probe} + E_{pump\perp}$ at five pump-probe delays -1.38ps < Δt < +1.3ps for He channels at ΔT=3ns, where $E_{pump\perp}$ represents the total component of the pump polarized orthogonal to its nominal incident polarization. With the exception of $\Delta t \simeq 0$, clear FDI fringes are visible along the λ-axis. However, compared to the reference interferograms with minimum $E_{leakage}$, the FDI fringes increased noticeably in amplitude and distorted in spatial structure, demonstrating that an additional field E_{depol}, produced through pump interaction with the channel, contributed to $E_{pump\perp}$ (i.e., $E_{pump\perp} = E_{leakage} + E_{depol}$). The interferograms have two important features: fringes are tilted, indicating an asymmetric x-dependent phase-front in $E_{pump\perp}$, and further, the direction of the tilt reverses on going from $\Delta t<0$ to $\Delta t > 0$ (see Fig. 2b), confirming its origin in the phase structure of $E_{pump\perp}$, and not an accidental misalignment of $E_{pump\perp}$ and E_{probe}. Since this feature was not observed in the FDI of two Gaussian pulses (obtained by intentionally rotating the incident pump polarization), we attribute it to the depolarization mechanism.

FDI fringe amplitude scaled in proportion to E_{pump} for I_{guided} down to $\sim 3 \times 10^{16}$ W/cm^2. The spatial phase structure of the interferograms also retained the qualitative features described above, suggesting that $E_{leakage}$ and E_{depol} scaled linearly with I_{guided}. Thus nonlinear Kerr rotation of the pump pulse appears not to contribute significantly to depolarization. Intensity independent polarization rotation of the pump in the channel can occur through mechanisms that occur in glass single mode fibers[25,26]. Perturbative solution of the wave equation in a parabolic channel
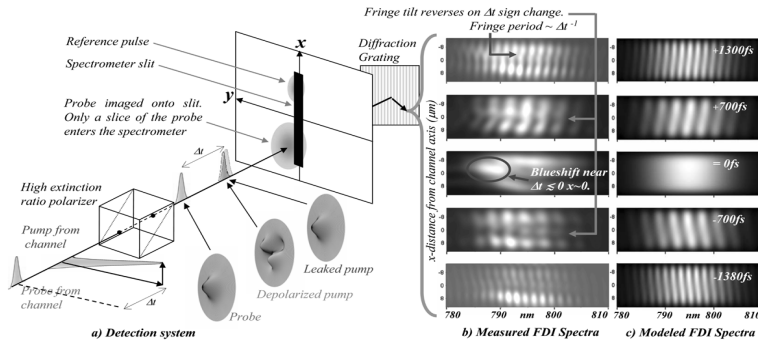

FIGURE 2. *a*) Schematic of the detection system, showing polarization of the fields E_{pump}, E_{probe}, E_{depol}, and $E_{leakage}$ relative to the spectrometer slit. Transverse mode structures of E_{probe}, E_{depol}, and $E_{leakage}$ are also shown. *b*) Example of single-shot, spatially resolved frequency-domain interferograms from He channels at several pump-probe time delays Δt (+1300fs to -1380fs). "$\Delta t \lesssim 0$" corresponds to probe moving at the leading edge of the pump. Note fringe tilt reversal as Δt changes sign, and small blue-shift (785nm – 790nm) near x = 0 at $\Delta t \lesssim 0$. *c*) Modeled FD interferograms obtained by interference of a Gaussian guided probe and the non-Gaussian depolarized component of the pump pulse produced in the $\sim$300μm channel end regions.

$[(\omega_p/\omega_{p0})^2=1+(r/r_{ch0})^2]$ shows that a hybrid mode is induced inside the channel. It has the form:

$$B_y(x,y,z)=B_0\frac{\omega_{p0}^2}{2\omega_0}\frac{xy}{r_{ch}^2}e^{\left[-\left(x^2+y^2\right)/2\sigma^2\right]}e^{(-i\Delta k\,z)}\left(1-e^{-i(\Delta k_1-\Delta k)z}\right) \qquad (1)$$

where $\sigma=(cr_{ch}/\omega_{p0})^{1/2}$ is the constant e^{-1} intensity radius of the guided pulse, $\Delta k=\omega_{p0}/k_0cr_{ch}\simeq15cm^{-1}$ is the change in k_0 for the guided mode, and $\Delta k_1=3\omega_{p0}/k_0cr_{ch}=3\Delta k$. The last term in (1) arises because the driving and depolarized components have slightly different phase velocities. As a consequence B_y does not grow monotonically with z, but fluctuates with period $(\Delta k_1-\Delta k)^{-1}\sim0.04cm\ll L_{ch}$ for our parameters. Because of this short coherence length the channel ends can dominate the depolarization process. The channel ends are narrower than the body of the channel and have higher plasma density. Physically reasonable numbers yield close estimate of the depolarized intensity. Fig. 2c shows FDI spectra modeled with the assumption that three pulses interfere: Gaussian probe, Gaussian leakage, and the above non-Gaussian mode. This model qualitatively reproduces the observed fringe tilt and tilt reversal about $\Delta t=0$ for parameters consistent with our experiments. (Details of this discussion are found in ref. 28).

At $\Delta t \lesssim 0$ FDI fringes were absent, but we observed blue-shifts of the channeled probe spectrum (Figs. 2b, 3b), even though blue-shifts were not detected in the transmitted pump (Fig.1, bottom right). The largest blue-shift ($\Delta\lambda_{probe}\sim 5\pm 1nm$) was observed with the probe in the leading edge of the pump (-50 < Δt < 0fs).
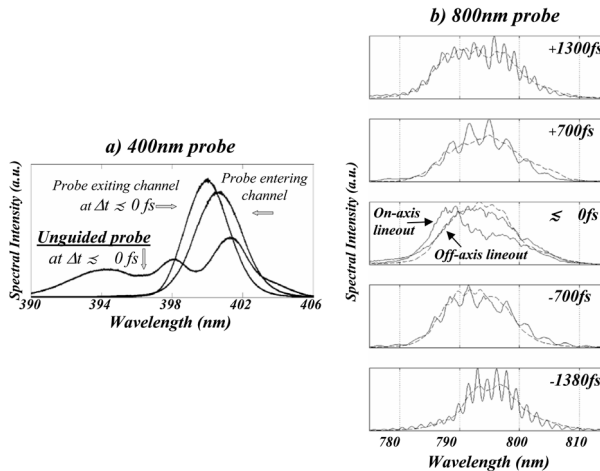

FIGURE 3. *a*) Single-shot, time resolved, spatially averaged, spectra of 400-nm probe: 1) entering the channel (reference spectrum); 2) exiting the channel; 3) propagating in 700-Torr He without channel (initial pump-probe delay was $\Delta t \lesssim 0$ in 2 and 3). Spectra of channeled 400-nm probes at delays other than $\Delta t \lesssim 0$ were unchanged. *b*) Lineouts of single-shot interferograms in Fig.2b (solid curves), compared with a split-off reference pulses that bypassed the channel (dashed curves). FDI and reference spectra coincide closely for all Δt except $\Delta t \lesssim 0$, where a blue-shift of $\Delta\lambda \sim 5nm$ is evident in the *on-axis* lineout of the channeled probe

The dependence of the blue-shifts on Δt identifies them as shifts in E_{probe}, because shifts in E_{depol} would not depend on Δt. The spatial dependence of the shift evident in Figs. 2b and 3b corroborates this conclusion. The blue-shifted portion of the detected spectrum (785-790 nm) is invariably concentrated on the channel axis (x=0 in Fig. 2b and on-axis lineout in Fig. 3b), where E_{probe} and E_{pump} are at maximum.

In order to quantify the blue-shift, transmitted probe spectra were compared to spectra of reference pulses that bypassed the channel. Fig. 3b superposes normalized lineouts (at fixed x and several Δt) of corresponding probe and reference spectra. The fits are very close in all cases except at $\Delta t \lesssim 0$. The prominent $\Delta t \lesssim 0$ blue-shift signifies ionization, by the leading edge of the pump, of residual unionized gas left after channel forms. Ionization fronts for both He^+ and He^{2+} indeed occur in the leading edge of the pump pulse, because their threshold intensities ($\sim 10^{15}$ and $\sim 10^{16}$ W/cm^2 for He^+ and He^{2+}, respectively)[24] are less than I_{guided}, and shift a relatively small fraction of the pump energy, producing undetectable changes in pump pulse. However, the probe pulse can "ride" the ionization front, shifting most of its energy, and producing a much larger blue shift. Thus the blue-shift of an appropriately timed probe pulse more sensitively characterizes residual ionization than the transmitted pump alone.

This measurement by itself does not pinpoint the location of the residual incompletely ionized gas. The greatest concentration is expected near the channel entrance and exit, where ionization by the channel-forming pulse is inefficient. Here the entering (exiting) pulse interacts with incompletely ionized gas at approximately full I_{guided} over path length $z \sim z_R \sim 250$ μm. On the other hand, once coupled into the channel, the pulse interacts with the plasma over path length $z \sim 60\, z_R$. Thus, since the probe blue-shift

$$\Delta\lambda_{probe} \approx z\lambda_{probe}^3 \frac{r_e}{2\pi c}\frac{dn_e}{dt} \qquad (2)$$

is proportional to z (r_e is the classical electron radius), ionization of residual gas ~ 60 x less dense than in the entrance (exit) region could cause an equivalent blue-shift. To distinguish these possibilities we repeated the experiment with a frequency doubled probe pulse in a channel identical to that used to measure the blue-shift of the 800 nm probe. The 400 nm probe walks off from the pump by approximately a pulse duration ($\tau_p = 80$fs) because of group velocity mismatch. Since the pump-induced ionization front is less than τ_p, any contribution from the channel transit to 400nm probe blue shift should be much reduced. Fig. 3a shows the measured blue-shifts: $\Delta\lambda_{400nm\text{-}probe} \simeq 0.8 \pm 0.2$ nm at $|\Delta t| \lesssim 0$. Within measurement error, these shifts are consistent with those observed with the 800 nm probe, scaled by the factor λ_{probe}^3. We must conclude that the 800 and 400 nm probes interact with the pump-induced ionization front over roughly equal path lengths that are shorter than the channel length, and the channel itself contributes relatively little to the observed blue-shift. This not only confirms previous conclusions about full ionization within the He channel,[7] but provides a much more stringent test than diagnostics based on the guided pump pulse or transverse channel interferometry.

CONCLUSION AND FUTURE WORK

Pump-probe measurements were implemented in ~1-cm-long plasma channel to characterize pump depolarization and ionization blue-shifting more sensitively than is possible with measurements of the pump pulse alone. The use of same wavelength (800nm) pump and probe pulses yields certain advantages over traditional two-color pump-probe experiments: first, frequency domain interferometry is simplified by employing only a single probe that interferes with a component of the pump (provided $\Delta t > \sim\pi/\Delta\omega$), second, group velocity matching is ensured throughout channel transit, and third, temporal calibration is trivial. In future experiments, we expect to use this form of phase-sensitive FDI method to measure index modulations with sensitivity of $\Delta n/n \sim 10^{-4}$ or better.

The use of an orthogonally polarized, same wavelength probe enables sensitive homodyne-characterization of the weak, depolarized component of the pump mode that is otherwise completely hidden by the main part of the intense pump. This technique allowed us to detect the depolarized component of a hybrid Gaussian pump pulse, and show its strongly non-Gaussian mode and a weak blue-shift fluctuating from shot to shot. In future experiments, this method can be reversed to sensitively measure non-Gaussian spatial structure changes of the probe (e.g., by pump induced wakefields) by FDI with the Gaussian pump leakage field of adjustable amplitude. In such experiments, $E_{leakage}$ would have to be much greater than E_{depol}, to ensure that $E_{leakage}$ is a closely Gaussian reference pulses. Nevertheless, subtle details of such measurements may require the consideration of the structure of E_{depol} determined here.

The comparison of results from same wavelength and two color pump-probe measurements yields information about the longitudinal location of ionization front induced index modulations. We have shown that the ionization blue-shifts cannot originate inside the plasma channel. These observations, and the supporting models, suggest that the depolarization and blue-shifting occur primarily at the channel ends.

We are currently working on a robust, damage resistant, differentially-pumped channel generation cell in which we can maintain repeatable, well controlled, uniform density, with sharp boundaries, and low exterior pressure. We have proceeded both experimentally and with the use of gas dynamic simulations to find the optimal size and materials for the entrance and exit apertures, to reach a compromise between pumping speed and damage threshold. The entrance of the cell is formed by a 2mm diameter central hole in the Axicon, into which we insert a tiny MACOR plug with interior diameter <1mm. The output window is formed by a fused silica window with a <2mm, heat polished aperture. If well aligned, this design operates indefinitely without damage with pump pulses at 10^{18} W/cm^2. The exterior pressure, in CW mode, can be maintained below 10Torr with interior pressure at 500Torr, and can be reduced to <1Torr in pulsed operation, while still allowing interior pressure equilibration. Measurements and simulations also confirm sub-mm boundary regions, that are critical for efficient and distortion free coupling.

ACKNOWLEDGMENTS

REFERENCES

1. P. Sprangle and B. Hafizi, *Phys. Plasmas* **6**, 1683-1689 (1999), and references therein.
2. Y. Ehrlich, C. Cohen, A. Zigler, J. Krall, P. Sprangle, E. Esarey, *Phys. Rev. Lett.* **77**, 4186 (1996).
3. D. Kaganovich, P. Sasorov, C. Cohen and A. Zigler, *Appl. Phys. Lett.* **75**, 772-774 (1999).
4. T. Hosokai, M. Kando, H. Dewa, H. Kotaki, S. Kondo, N. Hasegawa, K. Nakajima, and K. Horioka, *Opt. Lett.* **25**, 10-12 (2000).
5. A. Butler, D. J. Spence and S. M. Hooker, *Phys. Rev. Lett.* **89**, 185003 (2002).
6. C. G. Durfee III, J. Lynch and H. M. Milchberg, *Phys. Rev. E* **51**, 2368-2389 (1995).
7. E. W. Gaul, S. P. Le Blanc, A. R. Rundquist, R.Zgadzaj, H. Langhoff, and M. C. Downer, *Appl. Phys. Lett.* **77**, 4112-4114 (2000).
8. P. Volfbeyn, E. Esarey, W. P. Leemans, *Phys. Plasmas* **6**, 2269-2277 (1999).
9. S. P. Nikitin, I. Alexeev, J. Fan, and H. M. Milchberg, *Phys. Rev. E* **59**, R3839-R3842 (1999).
10. W. M. Wood, C. W. Siders, M. C. Downer, *Phys. Rev. Lett.* **67**, 3523-3526 (1991).
11. P. Blanc, P. Audebert, F. Fallies, J. P. Geindre, J. C. Gauthier, A. Dos Santos, A. Mysyrowicz, and A. Antonetti, *J. Opt. Soc. Am. B* **13**, 118-124 (1996).
12. M.K. Grimes, A.R. Rundquist, Y.-S. Lee, and M. C. Downer, *Phys. Rev. Lett.* **82**, 4010-4013 (1999).
13. K. Y. Kim, I. Alexeev, E. Parra and H. M. Milchberg, *Phys. Rev. Lett.* **90**, 023401 (2003).
14. C. W. Siders, S. P. Le Blanc, D. Fisher, T. Tajima, M. C. Downer, A. Babine, A. Stepanov, A. Sergeev, *Phys. Rev. Lett.* **76**, 3570-3573 (1996).
15. J. R. Marques, R. Dorchies, F. Amiranoff, P. Audebert, J. C. Gauthier, J. P. Geindre, A. Antonetti, T. M. Antonsen, P. Chessa, P. Mora, *Phys.Plasmas* **5**, 1162-1177 (1998).
16. S. P. Le Blanc, M. C. Downer, R. Wagner, S.-Y. Chen, A. Maksimchuk, G. Mourou and D. Umstadter, *Phys. Rev. Lett.* **77**, 5381-5384 (1996).
17. A. Ting, K. Krushelnick, C. I. Moore, H. R. Burris, E. Esarey, J. Krall and P. Sprangle, *Phys. Rev. Lett.* **77**, 5377-5380 (1996).
18. H. Kotaki, M. Kando, T. Oketa, S. Masuda, J. K. Koga, S. Kondo, S. Kanazawa, T. Yokoyama, T. Matoba, K. Nakajima, *Phys. Plasmas* **9**, 1392-1400 (2002).
19. S.P. Le Blanc, E.W. Gaul, N.M. Matlis, A.R. Rundquist, M.C. Downer, *Opt. Lett.* **25**, 764 (2000).
20. K. Y. Kim, I. Alexeev and H. M. Milchberg, *Appl. Phys. Lett.* **81**, 4124-4126 (2002).
21. S. C. Wilks, J. M. Dawson, W. B. Mori, T. Katsouleas, and M. E. Jones, *Phys. Rev. Lett.* **62**, 2600-2603 (1989).
22. J. M. Dias, L. Oliveira e Silva, and J. T. Mendonca, ``Photon accelerator and interferomety diagnostics of laser wakefields," in *Proceedings of the 1st JAERI-Kansai International Workshop on Ultrashort-Pulse Ultrahigh-Power Lasers and Simulation for Laser-Plasma interactions* ,JAERI-Conf. 98-004, 1997, pp. 1-24.
23. L. Lepetit, G. Cheriaux and M. Joffre, *J. Opt. Soc. Am. B* **12**, 2467-247 (1995).
24. S. Augst, D. Strickland, D. D. Meyerhofer, S. L. Chin, and J. H. Eberly, *Phys. Rev. Lett.* **63**, 2212 (1989).
25. W. K. Burns, Robert P. Moeller and Chin-lin Chen, *J. Lightwave Technol.* **LT-1**, 44-49 (1983).
26. Allan W. Snyder and John D. Love, *Optical Waveguide Theory*, Dordrecht, Kluwer Academic Publishers, 1983).
27. K. Y. Kim, I. Alexeev, J. Fan, E. Parra, and H. M. Milchberg, "Plasma waveguides: addition of end funnels and generation in clustered gases" in *Advanced Accelerator Concepts, Tenth Workshop*, edited by C. E. Clayton and P. Muggli, American Institute of Physics, 2002, pp. 646-653.
28. R. Zgadzaj, E. W. Gaul, N. H. Matlis, G. Shvets, and M. C. Downer, "Femtosecond pump-probe study of plasma channels", J. Opt. Soc. Am. B (To be published in 2004).